Fragment-Based Drug Design and Drug Repositioning Using Multiple Ligand Simultaneous Docking (MLSD): Identifying Celecoxib and Template Compounds as Novel Inhibitors of Signal Transducer and Activator of Transcription 3 (STAT3)

Huameng Li,[†] Aiguo Liu,[§,‖] Zhenjiang Zhao,[⊥] Yufang Xu,[⊥] Jiayuh Lin,[§] David Jou,[§] and Chenglong Li[*,†,‡]

[†]Biophysics Graduate Program, The Ohio State University, Columbus, Ohio 43210, United States

[‡]Division of Medicinal Chemistry & Pharmacognosy, College of Pharmacy, The Ohio State University, Columbus, Ohio 43210, United States

[§]Center for Childhood Cancer, Department of Pediatrics, College of Medicine, The Research Institute at Nationwide Children's Hospital, Columbus, Ohio 43205, United States

[‖]Department of Pediatrics, Tongji Hospital, Huazhong University of Science & Technology, Wuhan 430030, China

[⊥]State Key Laboratory of Bioreactor Engineering, Shanghai Key Laboratory of Chemical Biology, School of Pharmacy, East China University of Science and Technology, Shanghai 200237, China

ⓢ Supporting Information

ABSTRACT: We describe a novel method of drug discovery using MLSD and drug repositioning, with cancer target STAT3 being used as a test case. Multiple drug scaffolds were simultaneously docked into hot spots of STAT3 by MLSD, followed by tethering to generate virtual template compounds. Similarity search of virtual hits on drug database identified celecoxib as a novel inhibitor of STAT3. Furthermore, we designed two novel lead inhibitors based on one of the lead templates and celecoxib.

INTRODUCTION

New drug development still presents grand challenges. Conventional high throughput screening (HTS) drug discovery approach identifies many hits, but few of them can be developed into drugs. Currently, there are less than 1500 FDA-approved drugs. Poor efficacy and safety of hits are the major attritions of drug development. It is suggested that poor drug space, low structural diversity, and poor drug ADMET properties of compounds in HTS libraries may contribute to false positives and negatives. Over the past decade, fragment-based drug design (FBDD) has emerged as a successful alternative to drug discovery using biophysical methods like NMR and X-ray crystallography. For computational FBDD, conventional single fragment docking has problems of nonspecific binding and poor ranking power due to weak binding of small fragments. Recently, we have developed multiple ligand simultaneous docking (MLSD) to simulate the interplay of multiple molecules binding to the protein binding site(s).[1] In a test case, MLSD identified the correct binding modes of multiple fragments of drug lead 4-[4-[(4′-chloro[1,1′-biphenyl]-2-yl)methyl]-1-piperazinyl]-N-[[4-[[(1R)-3-(dimethylamino)-1-[(phenylthio)methyl]propyl]amino]-3-nitrophenyl]sulfonyl]benzamide (ABT-737)[1] in the respective subpockets of the binding groove of cancer target Bcl-xL, whereas single-fragment docking failed to do so because of energetic and dynamic coupling among the fragments.[2] The results suggest potential applications of MLSD to improve fragment-based docking screening. On the other hand, to reuse existing drugs for new targets, a drug repositioning concept has been proposed recently.[3] Previous analysis revealed that more than 30% of drugs share building blocks.[4] We hypothesize that FBDD using privileged drug scaffolds would help to generate lead compounds with improved ADMET properties.

To meet the challenge of drug discovery, we present here a novel approach for drug lead discovery using MLSD, drug scaffolds, and drug repositioning. Cancer target signal transducer and activator of transcription 3 (STAT3), an oncogene being constitutively activated in numerous cancers, was used as a test case in our study.[5−7] Currently there is no report of an approved drug to target STAT3, although a number of small molecule inhibitors of STAT3 have been discovered via HTS and virtual docking.[8−15] Figure 1 shows our drug discovery methodology. It proceeds as follows: (1) A small library of drug scaffolds is identified for the binding hot spots of STAT3 SH2 domain. (2) MLSD screening of the privileged drug scaffolds is then performed to identify optimal fragment combination-(s). (3) Linking of the fragment hits generates possible hit compounds as templates. (4) Similarity search of template compounds in drug databases identifies existing drugs as possible inhibitors of the protein target of interest.

RESULTS AND DISCUSSION

Identifying Privileged Drug Scaffolds for STAT3. It has been reported that the STAT3 pathway is activated upon the phosphorylation of tyrosine 705, followed by dimerization, nuclear translocation, and DNA binding. The druggable binding cleft of the STAT3 SH2 domain (PDB code 1BG1) consists of three subpockets: pTyr705 (pY705) binding site, Leu706 binding site (L706), and a side pocket (Ile597, Leu607, Thr622, and Ile634).
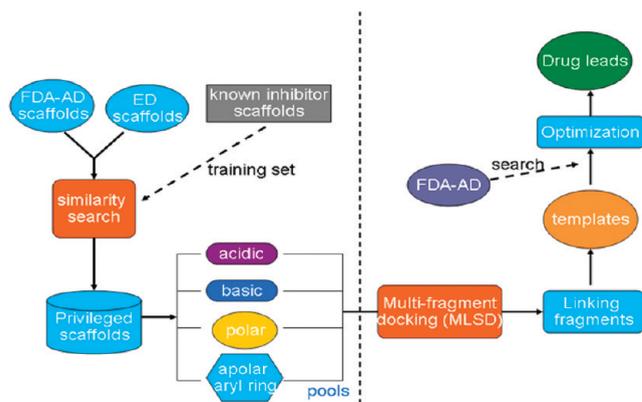
Figure 1. Scheme of drug discovery using MLSD and drug repositioning.

Figure 2. Privileged drug scaffolds for STAT3 SH2. Pool 1 is for pY705 site, and pool 2 is for L706 site or side pocket.

The main pTyr705 binding site is polar and basic, while the Leu706 and side pocket are hydrophobic. We built a small library of feature fragments from a collection of small molecule inhibitors of STAT3 SH2 in previous reports.[8−15] To avoid fragments with undesired drug ADMET properties, drug scaffolds structurally or chemically similar to the obtained feature fragments were identified by similarity search on a drug scaffold database. Figure 2 lists a small library of drug scaffolds identified, which were grouped into two pools: polar and nonpolar. The polar scaffolds in pool 1 favor binding to the polar and basic pY705 site, and the relatively nonpolar scaffolds in pool 2 are for the L706 site or side pocket.

Simultaneous Docking of Three Fragments to Binding Hot Spots of STAT3 SH2. So far, there has been no report of a fragment-based design approach to identify inhibitors of STAT3. Docking modeling showed that previously reported inhibitors bound to two of the three subpockets of the STAT3 SH2 domain. To improve binding affinity, we applied MLSD to dock multiple drug scaffolds in a concerted way to the three binding hot spots of STAT3, like fitting the right piece into the right place in jigsaw puzzle (Figure 3). Briefly, three drug fragments, one from pool 1 and the other two from pool 2, were used as inputs for the MLSD docking screening. The combination of drug scaffolds in the two pools generated a diverse set. Figure 3 shows that hits H1 (f1, f2, and f3) and H2 (f1, f4, and f5) docked to the hot spots of STAT3 SH2, with a predicted binding energy of −12.5 and −12.1 kcal/mol, respectively. In both hits, the polar fragment f1 (phenylsulfonamide) occupied the main
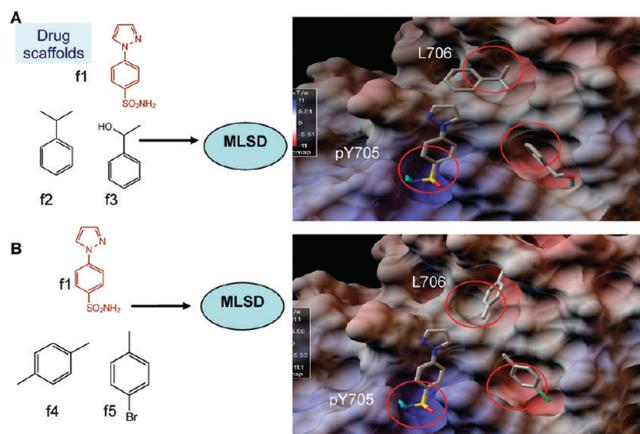
Figure 3. Scheme of MLSD screening of drug scaffolds for binding hot spots of STAT3 SH2. (A) In hit 1 (H1), fragments f1 (sulfonamide), f2 (1-phenylethanol), and f3 (2-phenylpropane) occupied the three hot spots (pY705, L706, and side pocket) of STAT3 with a binding energy of −12.5 kcal/mol. (B) In hit 2 (H2), fragments f1 (sulfonamide), f4 (1,4-dimethylbenzene), and f5 (1-bromo-4-methylbenzene) docked into three hot spots with a binding energy of −12.1 kcal/mol. Scaffolds are shown in stick-ball and colored by atom type.

pY705 binding pocket formed by surrounding residues Arg609, Lys591, Glu612, and Ser613. In hit H1, fragment f2 (1-phenyle-thanol) occupied the L706 subpocket and f3 (2-phenylpropane) docked to the side pocket. In hit H2, f4 and f5 bound to the L706 and subpocket, respectively.

Interestingly, predicted binding energies of hit H1 and H2 are very close. Further binding mode cluster analysis revealed that with similar binding energies, the binding modes of f2, f3, f4, f5 in the L706 and side pocket could be different and dynamic (Figure S2 of Supporting Information). The binding affinity of aromatic fragments f2 and f3 was similar to that of f4 and f5. Docking simulation results suggest that the polar pY705 site is essential and sulfonamide f1 moiety is a key fragment for binding. The docked fragments and their binding modes could be used as a blueprint to design possible inhibitors for STAT3. Our results show for the first time three fragments docked into the three hot spots of STAT3 SH2.

Linking Fragments for Hits and Virtual Template Compounds Design. To generate possible lead candidates, we linked the three fragments in hits H1 and H2 using different chemical tethers such as amide, amine, ether, and olefin. The structures of linked compounds and their docking energies are listed in Table S1 of Supporting Information. The virtual templates had docking binding energies in the range −8.2 to −12.0 kcal/mol. All 15 virtual compounds had relatively good binding to all three hot spots of STAT SH2 in docking modeling. Figure 4A shows the docking models of template compounds **T1** and **T2**. The top hit **T1** (green) demonstrated binding modes and binding energy ($\Delta G = -12.0$ kcal/mol) very close to that of the docked f1, f2, and f3 in hit H1 ($\Delta G = -12.5$ kcal/mol). Compound **T2** (red color) also bound relatively well to the three hot spots of STAT3, with binding modes similar to that of fragments f1, f4, and f5 in H2. The linked molecule **T2** gave a lower binding affinity compared to the three docked fragments (f1, f4, and f5) possibly because of the short linker between f1 and f5 in **T2**, which could lead to the tilt of f1 and shallow binding of f5. Also, the strain and single bond entropic penalty of linker upon binding compared to the free fragments could result in a weaker binding energy. We
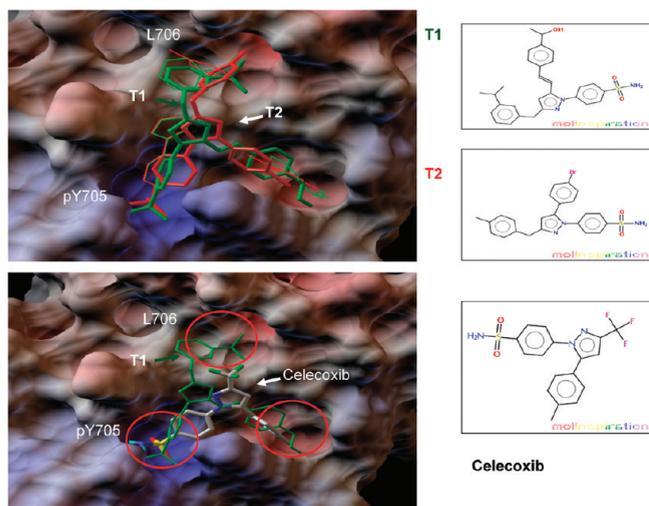
Figure 4. (A, top) Linking the docked fragments to obtain virtual template compounds. Tethering f1, f2, and f3 in hit H1 gave **T1** (green stick-ball), and linking f1, f4, and f5 of H2 generated **T2** (red stick-ball). Docked fragments of f1, f2, and f3 are represented by the thin green line, and f1, f4, and f5 are represented by the thin red line. Redocking of **T1** and **T2** to STAT3 resulted in binding energies of −12.0 and −8.6 kcal/mol, respectively. (B, bottom) Drug xelecoxib was identified as a novel inhibitor of STAT3 SH2 by similarity searching for **T1**, **T2**, and other virtual compounds in DrugBank. Docking of celecoxib (atomic coloring stick-ball) to STAT3 SH2 showed that phenylsulfonamide and phenyl-methyl bound to the pY705 site and side pocket, respectively.
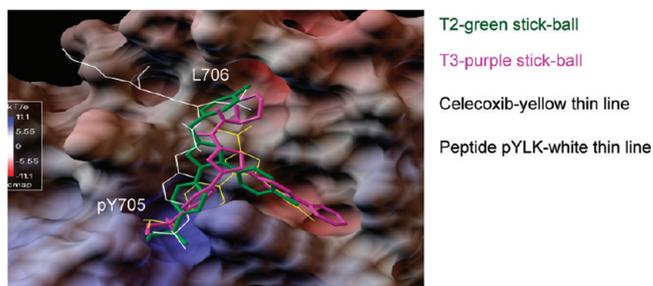
Figure 5. Docking modeling of celecoxib (yellow thin line), **T2** (green stick-ball), and **T3** (purple stick-ball) to STAT3. Native pTyr peptide (pYLK) binding is shown as a thin white line. Both compounds **T2** and **T3** have an extra hydrophobic group binding to the L706 site, which results in better binding energies of −8.6 and −9.2 kcal/mol, respectively, compared to celecoxib (−6.9 kcal/mol). The predicted binding modes and energies show good correlations with inhibition activities of celecoxib, **T2**, and **T3** on STAT3 in HCT-116 cell based assays.

found it is very difficult for a linked compound to exactly match binding modes and orientations of the docked fragments. One possible reason is that the docking simulation gives a cluster of binding modes with very similar binding energies. Fragment binding in the L706 and side pocket is dynamic to some degree as shown in Figure S2 of Supporting Information.

Drug Repositioning. The docked fragments define the blueprint and main pharmacophore of possible binders. This would enable us to search for template compounds on a drug database to match compounds with a similar binding pharmacophore. We performed a similarity search of all 15 template compounds on an FDA approved drug set in DrugBank.[17] Thirteen out of the 15 (87%) virtual
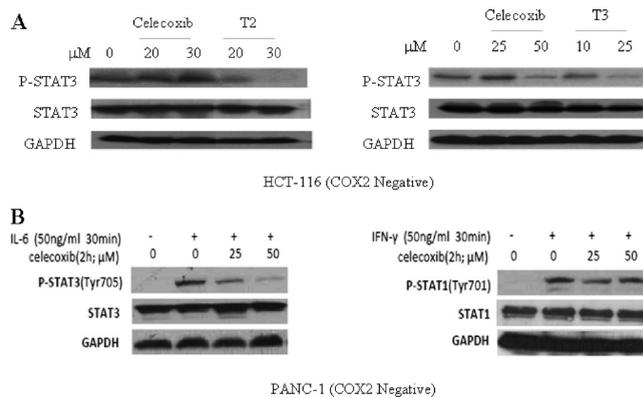
Figure 6. Selective inhibition of STAT3 by celecoxib, **T2**, and **T3**. (A) Celecoxib, **T2**, and **T3** inhibited STAT3 phosphorylation (Y705). Compounds **T2** and **T3** were more potent than celecoxib at inhibiting P-STAT3. (B) Celecoxib showed inhibition of STAT3 phosphorylation induced by IL-6 but not STAT1 phosphorylation by interferon-γ.

compounds identified celecoxib as a top hit (Tanimoto similarity coefficient of ≥0.6). Both **T1** and **T2** matched celecoxib as a top hit in DrugBank. Docking celecoxib to STAT3 SH2 resulted in a major binding cluster (80% probability), where the polar phenylsulfonamide occupied the pY705 site and nonpolar phenylmethyl occupied the side pocket (Figure 4B). In addition, docking modeling of celecoxib to STAT3 indicated that the binding modes and binding energy were comparable to most of the known inhibitors, which bound to the main pY705 site and only one of the L706 and side-pocket hot spots.[4−11] Docking celecoxib gave a lower binding affinity (−6.9 kcal/mol) than that of **T1** (−12.0 kcal/mol) and **T2** (−8.6 kcal/mol). Comparing binding modes of celecoxib with that of **T1** and **T2** indicates that the lower binding affinity is likely due to the missing third fragment in celecoxib for the L706 binding subpocket.

Virtual Hit Compounds T2 and T3 as More Potent Inhibitors of STAT3. To investigate whether binding to all three subpockets of STAT3 could improve inhibition on STAT3, template compounds were selected for synthesis based on ease of synthetic procedure and predicted binding modes and energies. The synthesis of top hit compound **T1** is challenging and the effort to synthesize it is ongoing. **T2** was synthesized. **T3** is an optimization of celecoxib to strengthen side pocket binding and to add L706 binding. The docking modeling of **T2** and **T3** shows that **T2** and **T3** bind relatively well to all three subpockets of STAT3 and can effectively compete with native phosphotyrosine peptide binding (Figure 5). Compared to celecoxib, **T2** and **T3** had better binding modes and an improved binding energy of −8.6 and −9.2 kcal/mol, respectively. The stronger binding is likely due to an extra fragment in **T2** and **T3** for binding to the L706 subpocket. The modeling would suggest that binding the L706 subpocket helps increase inhibition of STAT3. Cancer cell (HCT-116) assays also demonstrated that **T2** and **T3** are more potent inhibitors of STAT3 than celecoxib (Figure 6A and Table 1). The modeling results are consistent with the inhibition activities of celecoxib, **T2**, and **T3**.

Cancer Cell Line Assays: Celecoxib and T2 and T3 Down-Regulate STAT3 Phosphorylation in a Dose-Dependent Manner. The drug celecoxib is commonly known as a cyclooxygenase-2 (COX-2) inhibitor. To exclude interference of COX-2, human colon cancer cell line (HCT-116) that expresses constitutively activated STAT3 but not COX-2 was used in our study.[18−21] To examine the inhibition of STAT3 phosphorylation, a Western blot was performed to detect the amount of phosphorylated STAT3

Table 1. Docked Binding Energies and IC$_{50}$ of Celecoxib, T2, and T3 in HCT-116 Cell Viability Assays

compd	docking ΔG (kcal/mol)	IC$_{50}$ (μM)	binding mode	MW	CLogP	PSA (Å^2)
celecoxib	−6.9	43.3	pY705 and side pocket	381.4	3.6	78.0
T2	−8.6	9.7	pY705, L706, and side pocket	482.4	5.5	78.0
T3	−9.2	10.1	pY705, L706, and side pocket	501.6	3.2	110.3

(P-STAT3) after HCT-116 cells were treated with celecoxib, **T2**, and **T3** (10−50 μM). As shown in Figure 6, the amount of P-STAT3 decreased in HCT-116 cells with increasing doses of celecoxib, **T2**, and **T3**. STAT3 is phosphorylated through the gp130 cytoplasmic pTyr loop binding to the STAT3 SH2 domain; thus, blocking of STAT3 SH2 by inhibitors stops STAT3 phosphorylation. The expression of total STAT3 remained constant, which indicates that the decrease of P-STAT3 was not due to a constitutional decrease of total STAT3 protein. The results also show that **T2** and **T3** have more potent inhibitory effects on P-STAT3 than celecoxib (Figure 6A). This is consistent with the docking prediction.

Celecoxib Inhibits Interleukin-6 (IL-6) Induced STAT3 Phosphorylation but Not STAT1. We investigated whether celecoxib could inhibit IL-6 induced STAT3 phosphorylation in PANC-1 cancer cells. PANC-1 cells were cultured in serum free medium for 24 h and were pretreated with 25 or 50 μM celecoxib for 2 h. Then the cells were treated with 50 ng/mL IL-6 or interferon-γ for 30 min. We observed that celecoxib inhibited IL-6 induced STAT3 phosphorylation but had little effect on STAT1 phosphorylation induced by IFN-γ (Figure 6B).

Cell Viability Assay. Cell viability assay was used to measure inhibitory effects of celecoxib, **T2**, and **T3** on human colon cancer cells (HCT-116). The results are listed in Table 1. IC$_{50}$ values are as follows: celecoxib, 43.3 μM; **T2**, 9.7 μM; **T3**, 10.1 μM. **T2** and **T3** showed more potent inhibition of P-STAT3 than celecoxib. The results are consistent with the modeling prediction.

■ CONCLUSION

Our results show that combinations of three drug fragments found through MLSD bind to the three subpockets of STAT3 SH2. Linking of the docked fragments gave virtual hit compounds with potentially improved potency and ADMET properties. Similarity searching of virtual compounds in DrugBank identified celecoxib as a novel inhibitor of STAT3. Also, two novel hit compounds were designed to bind all three subpockets, which demonstrated more potent inhibition of STAT3 with IC$_{50}$ in the low micromolar range in HCT-116 cancer cell line assays. The proposed computational method, which uses privileged drug fragments, MLSD, and drug repositioning, can potentially be applied for drug discovery and fragment-based drug design for other targets.

■ EXPERIMENTAL SECTION

Privileged Drug Scaffolds Preparation for STAT3. The 436 drug scaffolds from FDA approved drugs (AD) as reported by Wang et al. were used for a drug scaffold database.[4] The top 50 AD scaffolds in the database covered 52.6% of all FDA approved drugs. To prepare the drug scaffold library for STAT3, a collection of known inhibitors of STAT3 in previous reports were used to generate a set of feature fragments for the binding hot spots of STAT3 SH2. These known inhibitors were fragmented by a retrosynthetic approach. Drug scaffolds for STAT3 were then identified by similarity search of the obtained feature fragments on drug scaffold database. The privileged drug scaffold library for STAT3 was used for multifragment docking screening.

Multifragment Docking Screening and Drug Repositioning. The crystal structure of STAT3 SH2 domain (PDB code 1BG1) was used as the receptor for docking. MLSD program was employed for multifragment docking.[1,16] Privileged drug scaffolds were used as fragments for MLSD screening. In multifragment docking, two or three fragments from the two pools of the drug scaffolds were used to probe binding subpockets of STAT3 SH2. Systematic multifragment docking screening with the combinations of drug scaffolds was ranked by the predicted binding energy. The docked fragments with a predicted binding energy of less than −8.2 kcal/mol (dissociation constant K_d in submicromolar range) were considered for further visual inspection of binding modes and selected as hits. Previously reported procedure and parameter settings were used for multifragment docking.[1] Lamarckian genetic algorithm (LGA) and particle swarm optimization (PSO) were used as a searching method depending on the dimensionality of search space. PSO, a searching method inspired by bird flocking, was used for MLSD with relatively high dimensions of conformational space. Virtual template compounds were obtained by linking docked fragments using various types of tethers. The candidates were optimized for drug properties: octanol−water partition coefficient (log P) and polar surface area (PSA). Drug properties were calculated using Molinspiration molecular property service (http://www.molinspiration.com). The linked compounds were redocked to STAT3 SH2 and ranked by binding energies and binding modes to generate hits. To apply the drug repositioning concept, similarity searches for template compounds in DrugBank (http://www.drugbank.ca/) were performed to identify potential drug analogues of hit compounds.[17] SMILES encoding and Tanimoto similarity coefficient cutoff of 0.5 were used for similarity search. The identified hit compounds were verified by computational redocking before selection for synthesis or purchase to perform cell line assays.

Cell Lines and Cell Culture. Human colon cancer cell line (HCT-116) and human pancreatic cancer cell line (PANC-1) were purchased from the American Type Culture Collection (ATCC). Cancer cell lines were cultured in DMEM medium supplemented with 10% FBS and 100 U/mL penicillin/streptomycin B, in a humidified 37 °C incubator with 5% CO$_2$.

Western Blot Analysis. HCT-116 cells were treated with Ccelecoxib, **T2**, and **T3** (10−50 μM) or DMSO control at 60−80% confluence in the presence of 10% fetal bovine serum (FBS) for 24 h and lysed in cold RIPA lysis buffer containing a cocktail of protease inhibitors to prepare whole-cell extracts.[11] Lysates were then centrifuged at 14 000 rpm for 10 min to remove insoluble materials. The 30−100 protein samples were separated by SDS−PAGE, transferred onto a PVDF membrane. After being blocked with 5% nonfat milk, the proteins were immunoblotted overnight at 4 °C with 1:1000 dilution of primary antibodies (Cell Signaling Technology) against phospho-STAT3 (pTyr705), STAT3, and GAPDH and 1:10000 dilution of HRP conjugated secondary antibody for 1 h at room temperature. The target proteins were visualized by chemiluminescence (Cell Signaling Technology).

Cell Viability Assay. HCT-116 cells were seeded in 96-well plates at a density of 3000 cells per well. Escalating concentrations (5−160 μM) of celecoxib and (1−75 μM) of **T2** and **T3** were added in triplicate to the plates in the presence of 10% FBS. The cells were incubated at 37 °C for 72 h. 3-(4,5-Dimethylthiazolyl)-2,5-diphenyltetrazolium bromide (MTT) viability assay was done according to the manufacturer's protocol (Roche

Diagnostics, Mannheim, Germany). The absorbance was read at 595 nm. Half-maximal inhibitory concentrations (IC_{50}) were determined using Sigma Plot 9.0 software (Systat Software Inc., San Jose, CA).

■ ASSOCIATED CONTENT

Ⓢ Supporting Information. Virtual docking results of template compounds, binding mode cluster of docked fragments, and synthesis of **T2** and **T3**. This material is available free of charge via the Internet at http://pubs.acs.org.

■ AUTHOR INFORMATION

Corresponding Author
*Phone: (614) 247-8786. Fax: (614) 292-2435. E-mail: Li.728@osu.edu.

■ ACKNOWLEDGMENT

■ ABBREVIATIONS USED

FBDD, fragment-based drug design; HTS, high throughput screening; MLSD, multiple ligand simultaneous docking; DAPI, 4′,6-diamidino-2-phenylindole; IL-6, interleukin 6; DMSO, dimethylsulfoxide; log P, octanol—water partition coefficient; PSA, polar surface area; STAT3, signal transducer and activator of transcription 3 (STAT3); ADMET, absorption, distribution, metabolism, excretion, and toxicity

■ REFERENCES

(1) Li, H.; Li, C. Multiple ligand simultaneous docking (MLSD): orchestrated dancing of ligands in binding sites of protein. *J. Comput. Chem.* **2010**, *31*, 2014–2022.

(2) Oltersdorf, T.; Elmore, S. W.; Shoemaker, A. R.; Armstrong, R. C.; Augeri, D. J.; Belli, B. A.; Bruncko, M.; Deckwerth, T. L.; Dinges, J.; Hajduk, P. J.; Joseph, M. K.; Kitada, S.; Korsmeyer, S. J; Kunzer, A. R.; Letai, A.; Li, C.; Mitten, M. J.; Nettesheim, D. G.; Ng, S.; Nimmer, P M; O'Connor, J. M.; Oleksijew, A.; Petros, A. M.; Reed, J. C.; Shen, W.; Tahir, S. K.; Thompson, C. B.; Tomaselli, K. J.; Wang, B; Wendt, M. D.; Zhang, H; Fesik, S. W.; Rosenberg, S. H. An inhibitor of Bcl-2 family proteins induces regression of solid tumours. *Nature* **2005**, *435*, 677–681.

(3) Chong, C. R.; Sullivan, D. J. New uses for old drugs. *Nature* **2007**, *448*, 645–646.

(4) Wang, J.; Hou, T. Drug and drug candidate building block analysis. *J. Chem. Inf. Model.* **2010**, *50*, 55–67.

(5) Bromberg, J. F.; Wrzeszczynska, M. H.; Devgan, G.; Zhao, Y; Pestell, R. G; Albanese, C; Darnell, J, E, Jr. Stat3 as an Oncogene. *Cell* **1999**, *98*, 295–303.

(6) Kortylewski, M; Kujawski, M; Wang, T; Wei, S; Zhang, S.; Pilon-Thomas, S.; Niu, G.; Kay, H.; Mulé, J.; Kerr, W. G.; Jove, R.; Pardoll, D.; Yu, H. Inhibiting Stat3 signaling in the hematopoietic system elicits multicomponent antitumor immunity. *Nat Med.* **2005**, *11*, 1314–1321.

(7) Costantino, L; Barlocco, D. STAT 3 as a target for cancer drug discovery. *Curr. Med. Chem.* **2008**, *15*, 834–843.

(8) Xu, X; Kasembeli, M. M.; Jiang, X; Tweardy, B. J.; Tweardy, D. J. Chemical probes that competitively and selectively inhibit Stat3 activation. *PLoS One* **2009**, *4* (3), e4783, DOI: 10.1371/journal.pone.0004783.

(9) Xu, J; Cole, D. C.; Chang, C. P.; Ayyad, R; Asselin, M; Hao, W; Gibbons, J; Jelinsky, S. A; Saraf, K. A.; Park, K. Inhibition of the signal transducer and activator of transcription-3 (STAT3) signaling pathway by 4-oxo-1-phenyl-1,4-dihydroquinoline-3-carboxylic acid esters. *J. Med. Chem.* **2008**, *51*, 4115–4121.

(10) Schust, J.; Sperl, B.; Hollis, A.; Mayer, T. U.; Berg, T. Stattic: a small-molecule inhibitor of STAT3 activation and dimerization. *Chem. Biol.* **2006**, *13*, 1235–1242.

(11) Song, H.; Wang, R.; Wang, S.; Lin, J. A low-molecular-weight compound discovered through virtual database screening inhibits Stat3 function in breast cancer cells. *Proc. Natl Acad. Sci. U.S.A.* **2005**, *102*, 4700–4705.

(12) Siddiquee, K; Zhang, S; Guida, W. C; Blaskovich, M. A; Greedy, B; Lawrence, H. R; Yip, M. L.; Jove, R; McLaughlin, M. M; Lawrence, N. J; Sebti, S. M.; Turkson, J. Selective chemical probe inhibitor of stat3, identified through structure-based virtual screening, induces antitumor activity. *Proc. Natl Acad. Sci. U.S.A.* **2007**, *104*, 7391–7396.

(13) Siddiquee, K. A; Gunning, P. T; Glenn, M; Katt, W. P.; Zhang, S.; Schrock, C.; Sebti, S. M.; Jove, R.; Hamilton, A. D.; Turkson, J. An oxazole-based small-molecule Stat3 inhibitor modulates Stat3 stability and processing and induces antitumor cell effects. *ACS Chem. Biol.* **2007**, *2*, 787–798.

(14) Bhasin, D.; Cisek, K.; Pandharkar, T.; Regan, N.; Li, C.; Pandit, B.; Lin, J.; Li, P. K. Design, synthesis, and studies of small molecule STAT3 inhibitors. *Bioorg. Med. Chem. Lett.* **2008**, *18*, 391–395.

(15) Lin, L; Hutzen, B; Li, P. K.; Ball, S.; Zuo, M; DeAngelis, S; Foust, E; Sobo, M.; Friedman, L.; Bhasin, D.; Cen, L; Li, C; Lin, J. A novel small molecule, LLL12, inhibits STAT3. Phosphorylation and activities and exhibits potent growth-suppressive activity in human cancer cells. *Neoplasia* **2010**, *12*, 39–50.

(16) Morris, G. M.; Goodsell, D. S.; Halliday, R. S.; Huey, R.; Hart, W. E.; Belew, R. K.; Olson, A. J. Automated docking using a Lamarckian genetic algorithm and an empirical binding free energy function. *J. Comput. Chem.* **1998**, *19*, 1639.

(17) Wishart, D. S.; Knox, C; Guo, A. C.; Cheng, D; Shrivastava, S; Tzur, D; Gautam, B.; Hassanali., M. DrugBank: a knowledgebase for drugs, drug actions and drug targets. *Nucleic Acids Res.* **2008**, *36* (database issue), D901–D906.

(18) Agarwal, B.; Swaroop, P.; Protiva, P.; Raj, S. V.; Shirin, H.; Holt, P. R. Cox-2 is needed but not sufficient for apoptosis induced by Cox-2 selective inhibitors in colon cancer cells. *Apoptosis* **2003**, *8*, 649–654.

(19) Molina, M. A.; Sitja-Arnau, M.; Lemoine, M. G.; Frazier, M. L.; Sinicrope, F. A. Increased cyclooxygenase-2 expression in human colon carcinomas and cell lines: growth inhibition by nonsteroidal anti-inflammatory drugs. *Cancer Res.* **1999**, *59*, 4356–4362.

(20) Wei, D.; Le, X.; Zheng, L.; Wang, L.; Frey, J. A.; Gao, A. C.; Peng, Z; Huang, S.; Xiong, H. Q.; Abbruzzese, J. L.; Xie, K. Stat3 activation regulates the expression of vascular endothelial growth factor and human colon cancer angiogenesis and metastasis. *Oncogene* **2003**, *22*, 319–329.

(21) Lin, L; Hutzen, B.; Zuo, M.; Ball, S.; Deangelis, S.; Foust, E.; Pandit, B.; Ihnat, M. A.; Shenoy, S. S.; Kulp, S.; Li, P. K.; Li, C.; Fuchs, J.; Lin, J. Novel STAT3 phosphorylation inhibitors exhibit potent growth-suppressive activity in colon and breast cancer cells. *Cancer Res.* **2010**, *70*, 2445–2454.